Heats of Formation of C6H5•, C6H5+, and C6H5NO by Threshold Photoelectron Photoion Coincidence and Active Thermochemical Tables Analysis

ARTICLE *in* THE JOURNAL OF PHYSICAL CHEMISTRY A · DECEMBER 2010

Impact Factor: 2.69 · DOI: 10.1021/jp107561s · Source: PubMed

3 AUTHORS, INCLUDING:

Branko Ruscic
Argonne National Laboratory
153 PUBLICATIONS **5,130** CITATIONS

JPCAFH

DECEMBER 23, 2010
VOLUME 114
NUMBER 50

pubs.acs.org/JPCA

THE JOURNAL OF PHYSICAL CHEMISTRY A

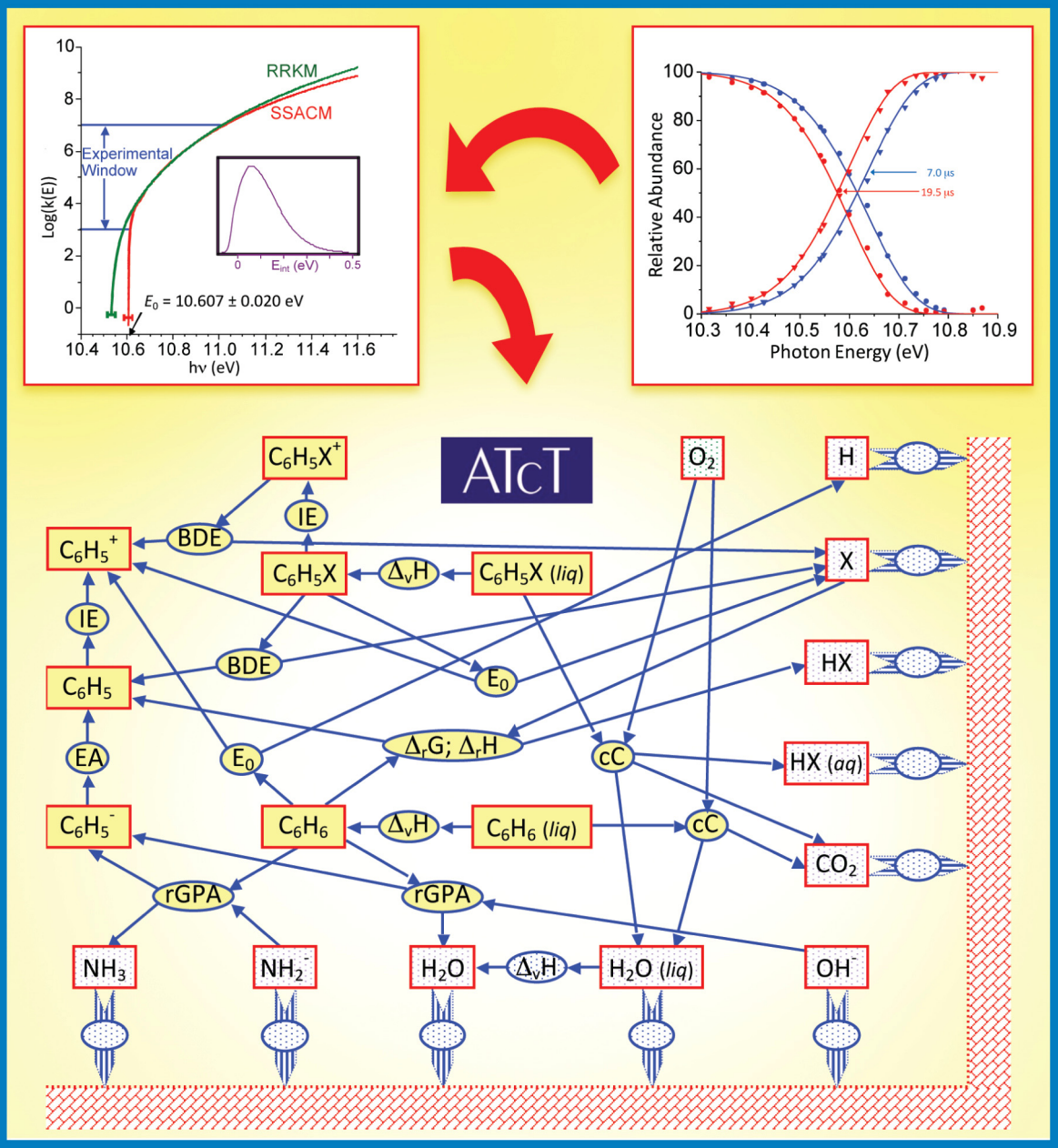

Synergism between Photoionization Measurements and Active Thermochemical Tables Producing New Thermochemistry of Phenyl
(see page 8A)

DYNAMICS, KINETICS, ENVIRONMENTAL CHEMISTRY, SPECTROSCOPY, STRUCTURE, THEORY

ACS Publications
High quality. High impact.

www.acs.org

Heats of Formation of $C_6H_5^{\bullet}$, $C_6H_5^+$, and C_6H_5NO by Threshold Photoelectron Photoion Coincidence and Active Thermochemical Tables Analysis

William R. Stevens,[†] Branko Ruscic,*[,‡,§] and Tomas Baer*[,†]

Department of Chemistry, University of North Carolina, Chapel Hill, North Carolina 27517, United States, Chemical Sciences and Engineering Division, Argonne National Laboratory, Argonne, Illinois 60439, United States, and Computation Institute, University of Chicago, Chicago, Illinois 60637, United States

Received: August 10, 2010; Revised Manuscript Received: October 27, 2010

Threshold photoelectron photoion coincidence has been used to prepare selected internal energy distributions of nitrosobenzene ions [$C_6H_5NO^+$]. Dissociation to $C_6H_5^+ + NO$ products was measured over a range of internal energies and rate constants from 10^3 to 10^7 s^{-1} and fitted with the statistical theory of unimolecular decay. A 0 K dissociative photoionization onset energy of 10.607 ± 0.020 eV was derived by using the simplified statistical adiabatic channel model. The thermochemical network of Active Thermochemical Tables (ATcT) was expanded to include phenyl and phenylium, as well as nitrosobenzene. The current ATcT heats of formation of these three species at 0 K (298.15 K) are 350.6 (337.3) ± 0.6, 1148.7 (1136.8) ± 1.0, and 215.6 (198.6) ± 1.5 kJ mol^{-1}, respectively. The resulting adiabatic ionization energy of phenyl is 8.272 ± 0.010 eV. The new ATcT thermochemistry for phenyl entails a 0 K (298.15 K) C−H bond dissociation enthalpy of benzene of 465.9 (472.1) ± 0.6 kJ mol^{-1}. Several related thermochemical quantities from ATcT, including the current enthalpies of formation of benzene, monohalobenzenes, and their ions, as well as interim ATcT values for the constituent atoms, are also given.

Introduction

The development of Active Thermochemical Tables (ATcT),[1,2] in which a multitude of directly measured reaction energy differences is used simultaneously to determine optimal heats of formations for the relevant species, has reinforced the importance of alternative thermochemical routes that relate the various species. In this study, we combine threshold photoelectron photoion coincidence (TPEPICO) studies and the ATcT approach while focusing on phenyl and phenylium. TPEPICO is used to examine the nitrosobenzene molecule, which dissociatively ionizes to form $C_6H_5^+$. The experimental determination of the appearance energy for this process, $E_0(C_6H_5^+/C_6H_5NO)$, in conjunction with prior measurements[3−6] of the neutral bond dissociation energy, $D_0(C_6H_5-NO)$, allows us to close the underlying positive ion thermochemical cycle and hence determine the adiabatic ionization energy of phenyl, IE(C_6H_5). The caveat is that monosubstituted benzenes are often difficult systems to study by dissociative photoionization ($C_6H_5X + h\nu \rightarrow C_6H_5^+ + X$) because of slow dissociation near threshold. However, as we shall show, ATcT can independently validate the measured onset(s) by furnishing values for $\Delta_fH°(C_6H_5^+)$, $\Delta_fH°(C_6H_5)$, and IE(C_6H_5) without any reference to determinations involving C_6H_5NO, after which it can be redeployed with full reference to those measurements, producing simultaneously an optimized enthalpy of formation of nitrosobenzene together with the best currently available values for phenyl and phenylium.

A precise ionization energy of the phenyl radical has been difficult to determine experimentally. Direct measurements are frustrated by poor Franck−Condon factors associated with the adiabatic transition from the ground electronic state of the radical to the ground singlet state of the phenyl ion. As a result, the two previously reported measurements of the adiabatic IE(C_6H_5) differ by >0.2 eV, well outside of their combined uncertainties.[7,8] At the same time, an indirect determination of IE(C_6H_5)–based on the difference in the heats of formation of phenyl and its cation–is hindered by serious difficulties in determining these two important thermochemical quantities with adequate accuracy and reliability. Suffice it to say that from the available experimental enthalpies of formation[7,9−35] (see Table 1), nearly any IE in the range 8.05−8.40 eV (with nominal uncertainties spanning ±0.05−0.22) appears possible, even after the unusually low value of $\Delta_fH(C_6H_5^+)$ obtained by Ripoche et al.[26] is excluded.

The first attempt to directly determine the IE(C_6H_5) was in 1972 by Sergeev et al.,[7] who used photoionization mass spectrometry to measure an 8.1 ± 0.1 eV ionization energy of phenyl radicals that were generated by pyrolysis of azobenzene. In 1987, Butcher et al.[8] reported an apparently more accurate onset of 8.32 ± 0.04 eV from photoelectron spectroscopy of phenyl radicals obtained by hydrogen abstraction from benzene with F atoms. However, plagued by weak intensity due to low concentrations of the radical on top of unfavorable Franck−Condon factors and, in addition, guided by ab initio computations of rather limited accuracy (at least by today's standards), Butcher et al. assigned the observed onset to the first excited $^3B_1$ state of the cation and contended that the adiabatic IE to the ground $^1A_1$ state of $C_6H_5^+$ is probably ∼8.0 ± 0.1 eV.

Attempts to clarify this issue by high-level theoretical methods have also been rather inconclusive. In 1997, using CCSD(T)/cc-pVDZ//B3LYP/cc-pVDZ and CCSD(T)/cc-pVDZ//MCSCF/6-31G** calculations on the phenyl radical and its cation, Hrusak et al.[36] obtained an IE of 8.1(±0.1) eV, identical to the experimental value of Sergeev et al.[7] and in reasonable agreement with the ∼8.0 eV estimate of Butcher et al.[8] However,

* To whom correspondence should be addressed. E-mail: ruscic@anl.gov (B.R.), baer@unc.edu (T.B.).
† University of North Carolina.
‡ Argonne National Laboratory.
§ University of Chicago.

10.1021/jp107561s
Published on Web 12/03/2010

TABLE 1: Literature Values for the Enthalpies of Formation of Phenyl and Phenylium[a]

species	0 K	298.15 K	uncertainty	ref
C_6H_5	*350.3*	337.0	±2.5	Alecu et al.[9]
	342.2	328.9	±4.2	Sivaramakrishnan et al.[10,11]
	350.1	336.8	±2.3	Ervin and DeTuri,[12] Blanksby and Ellison[13]
	351	338	±3	Heckmann et al.[14]
	352	339	±8	Tsang,[15] Robaugh and Tsang[16]
	352.7	339.7	±2.5	Davico et al.[17]
	341.4	330.1	±3.3	Berkowitz et al.[18]
	353.8	340.5	±11	Robaugh and Tsang[16]
	348.0	334.7	±8.4	Kiefer et al.[19]
	342.2	328.9	±8.4	McMillen and Golden[20]
	349	*336*	±12	Rosenstock et al.[21]
	338.4	325.1	±8.4	Chamberlain and Whittle,[22] Egger and Cocks[23]
	348.0	334.7	±5.4	Golden and Benson,[24] Rodgers et al.[25]
	350.6	337.3	±0.6	current work
$C_6H_5^+$	1085.7	*1074.0*	±7.5	Ripoche et al.[26]
	1148	*1136*	−	Lifshitz et al.[27]
	1141	*1129*	±10	Malinovich and Lifshitz[28]
	1133	*1121*	±5	Dannacher et al.[29]
	1130	*1118*	±5	Malinovich et al.[30]
	1135	*1123*	±5	Dunbar[31]
	1142	*1130*	±5	Dunbar and Honovich[32]
	1130	*1118*	±5	Rosenstock et al.[21]
	1133	*1121*	±5	Rosenstock et al.[21]
	1151	1167	±4	Rosenstock et al.[33]
	1146.4	*1134.7*	±4.2	Pratt and Chupka[34]
	1141	1130	±17	Beauchamp[35]
	1141.4	1129.7	±8.4	Sergeev[66]
	1148.7	1136.8	±1.0	current work

[a] All values are in kJ mol^{-1}. The values in italics have not been explicitly given in the quoted references and were obtained by converting from 298.15 to 0 K (or vice versa) using the currently adopted partition functions.

Hrusak et al.[36] also computed that the triplet state of the cation is ~0.8 eV above the ground state, which implies that the assignment of the 8.32 eV feature by Butcher et al.[8] as belonging to the $^3B_1$ state of $C_6H_5^+$ is rather unlikely. At about the same time, using the G2(MP2,B3LYP,RCC) composite approach that was modified by employing RCCSD(T) instead of UCCSD(T), Nicolaides et al.[37] have computed a higher IE of $8.2_1 \pm 0.1$ eV, nearly exactly midway between the two experimental results. More recently, Lau and Ng[38] calculated a value of 8.261 eV for IE(C_6H_5) with an estimated uncertainty of ±0.035 eV by CBS extrapolation using the CCSD(T)/CBS//CCSD(T)/6-311++G method. This value overlaps within the error bars the feature observed at 8.32 ± 0.04 eV by Butcher et al., yet is outside the uncertainty of the value 8.1 ± 0.1 eV of Sergeev et al. and well outside the estimated onset of 8.0 ± 0.1 eV by Butcher et al. Clearly, the ionization energy of phenyl merits further study.

Figure 1 demonstrates how IE(C_6H_5) can be determined from the positive ion thermochemical cycle that involves the neutral bond dissociation energy at 0 K, $D_0(C_6H_5-NO)$, and the phenyl ion appearance onset, $E_0(C_6H_5^+/C_6H_5NO)$, from the same C_6H_5NO precursor. This approach has the advantage that the derived IE(C_6H_5) is not dependent upon the benevolence of Franck−Condon factors or the accuracy of the available thermochemistry of the phenyl radical and its ion, though it does depend rather critically on the accuracy and reliability with which the two dissociation onsets can be determined.

The $E_0(C_6H_5^+/C_6H_5NO)$ can be in principle determined by photoelectron−photoion coincidence spectroscopy. The caveat is that the heterolytic dissociation to the phenyl ion from C_6H_5NO is immeasurably slow at the threshold, requiring an extrapolation that uses unimolecular rate theory to determine

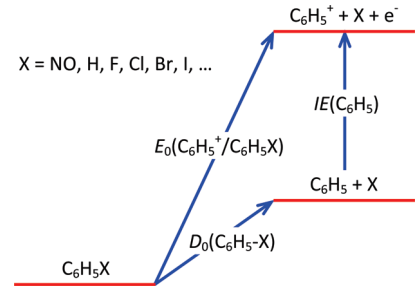

Figure 1. Energy diagram showing that the phenyl radical ionization energy is the difference between the onsets for C_6H_5 and $C_6H_5^+$.

$E_0(C_6H_5^+/C_6H_5NO)$. It has recently been shown that for the dissociation of benzene, butylbenzene, and halobenzene cations, which also have immeasurably slow rate constants at the threshold and no well-defined transition state, the extrapolated 0 K dissociation onset (E_0) depends strongly on the rate model used.[39,40] For these systems Rice−Ramsperger−Kassel−Marcus (RRKM) theory, although capable of fitting the data over 4−5 orders of magnitude, significantly underestimates E_0, while phase space theory (PST) does not fit the data very well and tends to overestimate E_0. On the other hand, a semiempirical variational transition state theory (VTST)[41] and the simplified statistical adiabatic channel model (SSACM)[42,43] are both capable of fitting the data and predicting the correct onset. Of these, the SSACM was found to be much easier to employ and is used here. More recent studies[44,45] have successfully employed this model to extrapolate accurate E_0 for both kinetic and competitive shifts.

The other ingredient required to close the positive ion cycle in Figure 1 is the neutral bond dissociation energy of nitrosobenzene. This has been reported by Park et al.[3] to be 226.8 ± 2.1 kJ mol^{-1} (54.2 ± 0.5 kcal mol^{-1}) at 0 K. While this value appears to be sufficiently accurate for the present purpose (limiting the accuracy of the inferred IE of phenyl to ≥±0.022 eV), one needs to take note of the fact that prior kinetic studies (Horn et al.[5] and Choo et al.[6]) have produced significantly lower values.

In order to sidestep the possibility of concealed systematic problems in the determined $E_0(C_6H_5^+/C_6H_5NO)$ and/or the available value(s) of $D_0(C_6H_5NO)$, either of which would adversely affect the resulting IE(C_6H_5), we employ the Active Thermochemical Tables approach in two discrete steps. The goal of the first step is to corroborate the measured $E_0(C_6H_5^+/C_6H_5NO)$ by independently validating the IE(C_6H_5) obtained from the positive ion cycle depicted in Figure 1 via determining the ATcT enthalpies of formation of phenyl and its ion. The necessary degree of independence during the validation step is attained by excluding from the ATcT thermochemical network any determinations involving C_6H_5NO. The second ATcT step is geared to make full use of the additional knowledge provided by the current measurement of E_0 and prior measurements of the homolytic bond dissociation energy of nitrosobenzene and obtain an optimized enthalpy of formation of C_6H_5NO together with the best currently available values for $\Delta_fH°(C_6H_5)$ and $\Delta_fH°(C_6H_5^+)$.

Active Thermochemical Tables. Active Thermochemical Tables are a novel approach that transcends the fundamental limitations that are engrained in the traditional sequential approach to thermochemistry (A begets B, which begets C...) by constructing, analyzing, and solving the underlying thermochemical network (TN).[1,2,46−49] This network does not contain enthalpies of formation of the target chemical species per se; rather, the TN stores the interdependencies between species in

the form of thermochemically relevant determinations, such as reaction enthalpies, bond dissociation energies, equilibrium constants, etc. These are entered in a form that is as close as possible to the thermochemical quantity that was actually measured, i.e., devoid of influences exerted by external data (auxiliary enthalpies of formation, partition function-related data such as entropies or enthalpy increments, etc.) Thus, for example, a study of the forward and reverse kinetic rates of a hydrogen abstraction by a halogen atom X from some species RH is not entered in the TN as a new measurement of the enthalpy of formation of the resulting radical R, nor even as a new determination of the R−H bond dissociation energy. Instead, it is entered either as the third law Gibbs energy or the second law enthalpy (or both, if appropriate) of the actually studied reaction RH + X → R + HX, typically at the midtemperature of the common range of validity of the forward and reverse rate constants. Similarly, an electronic structure computation is not entered as a newly computed enthalpy of formation, but as the computed atomization energy or as the appropriate isogyric/isodesmic/homodesmotic/etc. reaction. Not less importantly, each determination included in the TN is accompanied by an uncertainty that attempts to reflect its 95% confidence limit (which is the standard level of expression of uncertainties in thermochemistry,[50,51] as followed by virtually all existing thermochemical tables). In most cases, the above-described strategy of explicitly exposing all dependencies in the TN and preventing the deliberate introduction of "optimistic" uncertainties can be successfully achieved only by reinterpreting, refitting, reevaluating, and/or reverse engineering the measured data and the associated uncertainties, providing that sufficient information was presented by the original authors.

The Core (Argonne) Thermochemical Network, C(A)TN, is the central TN from which ATcT derives its thermochemical knowledge. C(A)TN currently encompasses over 900 chemical species containing H, O, C, N, and halogens, interconnected by more than 13 000 thermochemically relevant determinations. The ATcT results presented in this study are based on the two most recent versions of C(A)TN, which include the measurements relevant to defining the thermochemistry of phenyl and its positive and negative ions (ver. 1.108) as well as nitrosobenzene (ver. 1.110).

Experimental Methods

Threshold Photoelectron-Photoion Coincidence (TPEPICO). Experimental time-of-flight (TOF) distributions and breakdown diagrams were obtained using the TPEPICO technique that has been described in detail elsewhere,[40,52−54] and only a brief description is given here. The room temperature sample entered the ion source region of a time-of-flight mass spectrometer through a stainless steel needle where vacuum ultraviolet (VUV) light emitted from an H_2 discharge lamp dispersed by a 1 m normal incidence monochromator ionized the sample. The width of the entrance and exit slits was 100 μm, providing a resolution of 1 Å (8 meV at 10 eV). The wavelength was calibrated using the Lyman-α emission line. Upon ionization, an extraction field of 20 V cm^{-1} accelerated electrons and ions in opposite directions. Velocity focusing optics directed electrons having zero velocity perpendicular to the extraction axis onto a 1.4 mm aperture at the end of a 12 cm electron drift region, where they were detected by a Burle channeltron detector. A second channeltron detector collected the background signal of energetic electrons in order to subtract the contamination from energetic electrons with velocity toward the detector. The resolution of the photon monochromator limited the threshold energy resolution.

The dissociation rates of NO loss from nitrosobenzene ions near the dissociation limit are very low, so that no fragment ions can be observed at the dissociation threshold. Thus, to measure this threshold, we need to measure the dissociation rate constants as a function of the ion internal energy and then to extrapolate these rates to the dissociation limit. Metastable nitrosobenzene ions can dissociate anywhere between their birth up to the ion detector. During the first 7 μs ions accelerate in the 20 V cm^{-1} field over 5 cm to 100 eV. Slow dissociation in this acceleration region results in asymmetric fragment ion time-of-flight distributions. A second acceleration region, terminated by grids, increased the ion energy to 250 eV. After traversing a 25 cm long drift tube, a deceleration to 160 eV slowed down fragment ions produced in the long drift region more than parent ions and thus allowed us to separate these fragment ions from their parent ions. As shown in a previous publication,[40] fragment ions that are produced while passing through the 25 cm long drift region appear in a peak after the parent ion. The ion time-of-flight (TOF) was measured using a time-to-pulse height converter (TPHC) with the electron signal as the start and the ion signal as the stop. The TPHC signal from each electron-ion coincidence event was recorded by a multichannel pulse height analyzer (MCPHA), thus providing a TOF spectrum. A similar spectrum was collected with the energetic electron detector. Typical acquisition times for TOF distributions varied from 1 to 72 h.

Threshold Photoelectron Spectroscopy (TPES). A threshold photoelectron spectrum was taken at the VUV beamline of the Swiss Light Source (SLS) synchrotron at the Paul Scherrer Institut using the recently built imaging photoelectron−photoion coincidence (iPEPICO) experiment.[55] The sample is introduced effusively and is ionized by incident light from a 10 m in-line monochromator with 2 meV resolution at 15.760 eV. Electrons are velocity-focused onto a Roentdek imaging detector. Threshold electron counts are monitored as a function of photon energy to generate a TPES.

Computational Methods

All auxiliary electronic structure computations were performed using the Gaussian 03 code.[56] Rotational constants and vibrational frequencies that were needed for the statistical modeling of the experimental data were obtained at the B3LYP/6-311++G** level of theory. The modeling of unimolecular decay rates also required as input a reasonable value for the ionization energy of the nitrosobenzene parent molecule, IE(C_6H_5NO), which was obtained by combining experimental observations with CBS−APNO computations (vide infra).

Results and Discussion

Initial ATcT Thermochemistry and Energetics. The initial ATcT values for the enthalpies of formation of phenyl and phenylium, based on C(A)TN ver. 1.108, were $\Delta_f H°_0(C_6H_5) = 350.6 \pm 0.6$ kJ/mol and $\Delta_f H°_0(C_6H_5^+) = 1148.8 \pm 1.0$ kJ mol^{-1} at 0 K (337.3 and 1136.9 kJ/mol at 298.15 K), resulting in IE(C_6H_5) = 8.274 ± 0.011 eV. The related 298 K enthalpy increments, $[H°_{298}-H°_0](C_6H_5) = 14.19$ kJ mol^{-1} and $[H°_{298}-H°_0](C_6H_5^+) = 15.57$ kJ mol^{-1} are based on RRHO treatment of experimental vibrational fundamentals conveniently tabulated by Jacox[57] (for phenyl, see, in particular, Friderichsen et al.[58] and Radziszewski et al.[59]), and complemented by scaled[60] B3LYP/6-31G(2df,p) frequencies (from G3X computations).

We note parenthetically that the quoted uncertainty in the ATcT value for IE is based on the full covariance matrix. As a result, it is slightly smaller than the uncertainty that would be

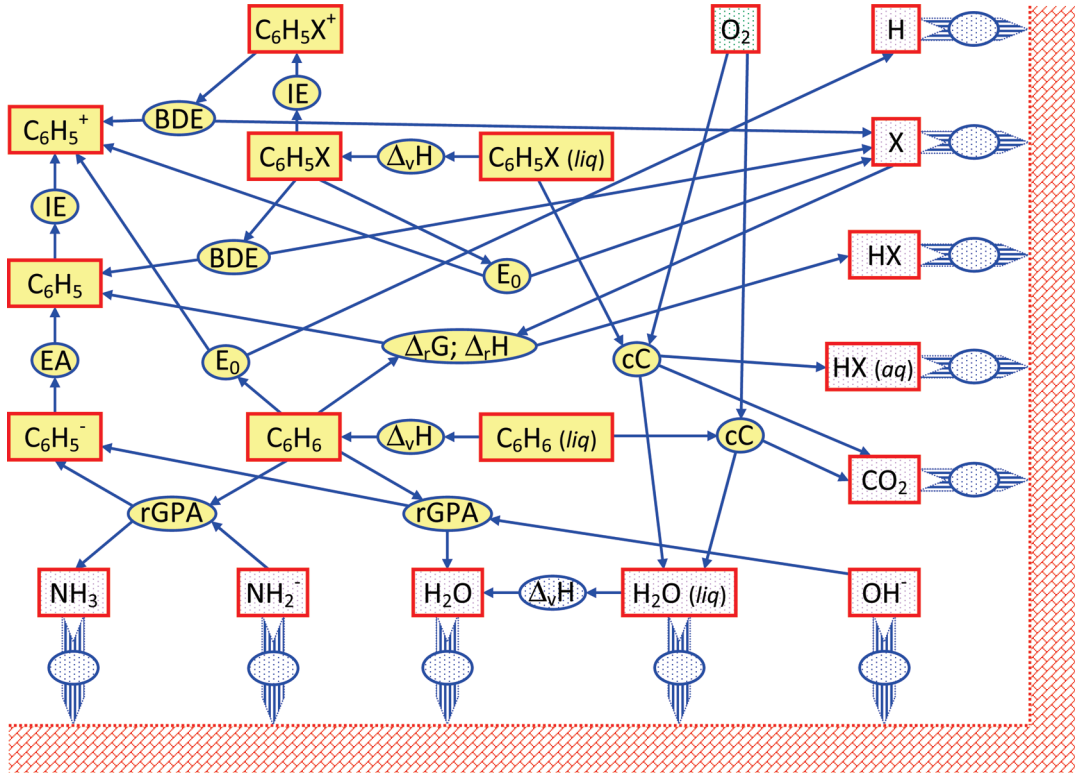

Figure 2. A graphical representation of a subset of the current thermochemical network illustrating the thermochemical topology of the species targeted in the present work. In the graph-theoretical sense, the TN contains primary (rectangles) and secondary (ovals) vertices. The primary vertices are the enthalpies of formation of targeted chemical species (gas-phase, unless noted otherwise), while the secondary vertices are actual thermochemically relevant determinations, such as adiabatic ionization energies (IE), adiabatic electron affinities (EA), bond dissociation enthalpies (BDE), photoionization fragment appearance energies (E_0), Gibbs energies and enthalpies of reaction ($\Delta_r G$ and $\Delta_r H$), vaporization enthalpies ($\Delta_v H$), combustion calorimetry measurements (cC), and relative gas-phase acidities (rGPA). The edges (arrows) are directed and weighted, reflecting the underlying stoichiometry. In order to avoid graphical congestion, the depiction of the TN was simplified by lumping the targeted monosubstituted benzenes into a generic primary vertex (C_6H_5X) and by leaving out several less prominent secondary vertices. The primary vertices at the bottom and at the right edge of the figure are anchored via numerous secondary vertices to the remainder of the TN (which currently contains >900 primary and >13000 secondary vertices). The primary−secondary−another primary connections are terminated only when encountering a primary vertex that represents an element in its reference state (such as O_2 in the upper right).

obtained from an error propagation scheme that ignores the off-diagonal element(s) of the covariance matrix (square root of the straightforward sum of squares), because the enthalpies of formation of phenyl and phenylium are mildly correlated (correlation coefficient $\rho = 0.20$). At the same time, the fact that $\rho \ll 1$ indicates that the ATcT enthalpies of formation of phenyl and phenylium have a quite significant degree of independence; i.e. it shows that the underlying ATcT statistical analysis ends up placing relatively little faith in the direct determinations of IE(C_6H_5) that were incorporated in the thermochemical network (experimental from Sergeev et al.[7] and Butcher et al.[8] and theoretical from Lau and Ng[38]) and, instead, ends up relying heavily on *other* thermochemically relevant knowledge in the TN relating to phenyl and phenylium (see Figure 2). The pertinent knowledge comes in the form of a number of experimental determinations, such as the third law measurement of the relative gas phase acidity (GPA) of benzene vs ammonia by Davico et al.,[17] the third and second law measurement of the relative GPA of benzene vs water by Meot-Ner et al.,[61,62] the adiabatic electron affinity of phenyl by Gunion et al.,[63] the third law Gibbs energy and the second law enthalpy of abstraction of hydrogen from benzene using chlorine atoms as resulting from the study by Alecu et al.[9] of the forward and reverse kinetic rate constants (and therefore the equilibrium constant), and the third law Gibbs energy of the same reaction that can be obtained by pairing up the forward rate constant of Sokolov et al.[64] with the reverse rate constant determined by Alecu et al.[9] C(A)TN also includes a number of kinetic studies in which the second law reaction enthalpy was obtained from the activation energy of the forward rate constant, while assuming that the reverse activation energy is close to zero (within the assigned uncertainty), such as the study of the bond dissociation enthalpy (BDE) of benzene by Kiefer et al.[19] and the studies of the reaction of trifluoromethyl with benzene by Chamberlain et al.[22] and Fielding and Pritchard.[65] Also included in C(A)TN is the threshold for the C−H bond fission of benzene cation obtained by Troe et al.[39] using the statistical adiabatic channel model and the appearance energies of $C_6H_5^+$ from halobenzenes obtained recently by Stevens et al.[40] using VTST and SSACM, as well as a number of older studies of the same processes, such as those by Sergeev et al.,[66] Rosenstock et al.,[21,33] Pratt and Chupka,[34] Durant et al.,[67] Lifshitz and Malinovich,[68] Malinovich et al.,[28,30] Dunbar,[31] Dunbar and Honovich,[32] and Stanley et al.,[69] together with earlier studies of the bond dissociation energy in halobenzenes by Rodgers et al.[25] and Ladacki and Szwarc.[70] Since several of the appearance energies of $C_6H_5^+$ have been determined relative to the ground state of the (halo)benzene cation (rather than the neutral), C(A)TN likewise includes a number of representative measurements of the ionization energies of benzene and halobenzenes.[29,66,67,71−119]

Finally, C(A)TN also includes a select subset of theoretical studies. For most gaseous species, the initial skeletal description that eases their introduction into the C(A)TN and provides us with an initial outlook of their structure, stability, expected

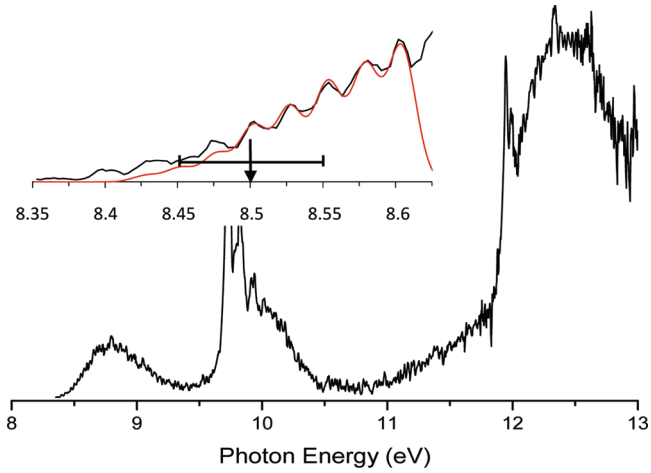

Figure 3. TPES of nitrosobenzene at the IE. (Inset) The black line corresponds to the experimental TPES, and the red line is a linear combination of Gaussians used to fit the TPES assuming that the IE is at the CBS−APNO value of 8.50 ± 0.08 eV (indicated in the inset by an arrow).

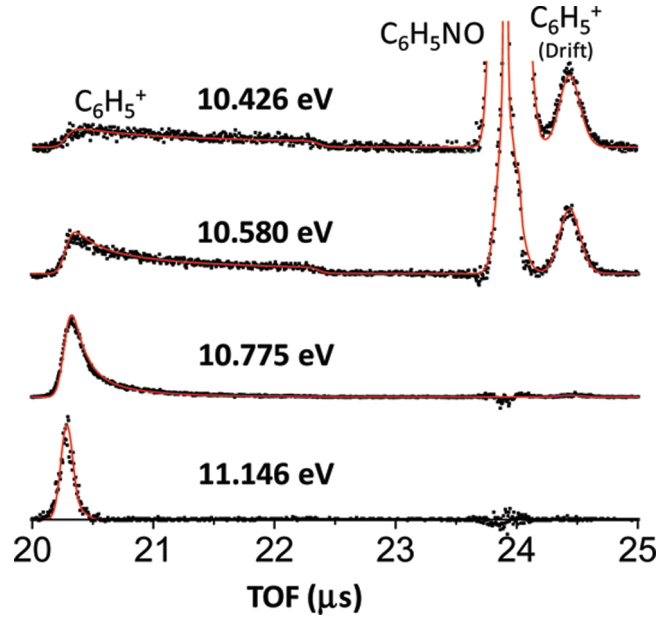

Figure 4. TOF distributions for nitrosobenzene over the experimental window. Black dots represent the experimental TOF distributions that have been corrected for ions that generated energetic electrons. Red lines indicate simulated TOF distributions. The asymmetric $C_6H_5^+$ peak between 20.2 and 22.2 μs is a result of ion fragmentation in the first acceleration region. Those fragment ions born in the drift region appear at 24.5 μs.

values of spectroscopic constants, etc., routinely relies on a series of standard composite electronic computations, which include G3,[120] G3B3,[121] G3X,[122] CBS-Q,[123] CBS-QB3,[124] CBS-APNO,[125] W1U,[126,127] and occasionally others. These computations were, in fact, used for the initial definition of phenylium and phenide in the TN, but they were *not* included in the case of phenyl, since it quickly became rather obvious that the very substantial spin contamination that occurs for phenyl (for the UHF, UMP2, UMP4, UQCISD, and UCCSD wave functions that are used in various steps of the G*n* and CBS-*xyz* sequences, $\langle S^2 \rangle$ ranges between 1.21 and 1.44 instead of the expected 0.75 for a doublet state) seriously compromises the outcome of these computations, resulting in a radical that is rather systematically insufficiently stable. The spin contamination problem in phenyl has been quite recently extensively discussed by Karton et al.,[128] who carried out W2.2 and W3.2lite computations. The latter results, which rely on ROHF wave functions for most (though not all) coupled cluster computations, were included in the C(A)TN, albeit the uncertainties originally declared by Karton et al. (±1.7 kJ mol^{-1} for the W3.2lite atomization energy) were guardedly augmented (to ±2.5 kJ mol^{-1} for the same). Also included in the C(A)TN were the G2(MP2,B3LYP,RCC) results of Nicolaides et al.[37] and the ROCBS-QB3 results of Wood et al.,[129] both of which use restricted-open wave functions that are immune to spin contamination.

Experimental Results. Figure 3 shows the threshold photoelectron spectrum for C_6H_5NO. A detail of the first band shows some vibrational structure with a spacing of 205 cm^{-1} that we ascribe to a single vibrational mode. The reason for this is that if two or more modes had significant Franck−Condon factors for $\Delta v > 1$ transitions, the structure would disappear due to dephasing of the two (or more) slightly different vibrational modes. The calculated vibrational level spacing for the neutral and ionic C−N−O bending mode is close to the observed spacing between the peaks in the TPES. This vibrational frequency of this mode changes from 257 cm^{-1} in the neutral molecule to 221 cm^{-1} in the ion, and the C−N−O bond angle changes from 116° to 134°, which makes it a likely mode to be excited. The low value of these bending modes makes the presence of hot bands likely, which means that it is difficult to determine the 0−0 origin of this vibrational progression. We therefore rely upon the IE predicted using CBS−APNO to be 8.50 ± 0.08 eV. As a check, we have taken a linear combination of Gaussian functions with widths and centroids optimized to fit the experimental TPES. The coefficients were determined by assuming that each peak corresponds to a single transition (i.e., the peaks at 8.475 and 8.525 eV are due solely to the $v_1 \rightarrow v_0^+$ and $v_0 \rightarrow v_1^+$ transitions, respectively) and that the Franck−Condon factors for $v_i \rightarrow v_j^+$ transitions are equal to $v_j \rightarrow v_i^+$ transitions. This allows us to predict the intensity of the hot bands independent of the Franck−Condon factors by taking the ratio of the $v_i \rightarrow v_j^+$ peak intensity to the $v_j \rightarrow v_i^+$ intensity. The results from this approach are shown in the inset of Figure 3. It is observed that this method somewhat underestimates the hot band intensities, which may be due to the assumption that each peak corresponds to a single transition. Performing a similar analysis assuming a higher energy IE results in a worse fit while a lower IE results in a better fit to the TPES. However, it is not clear whether this is due to an incorrect IE assignment, simplifying assumptions in the model, or the fact that at lower IE's the fit is less sensitive. A more sophisticated analysis of the TPES may eliminate this ambiguity, but that is outside of the scope of this paper. We account for the uncertainty in the IE(C_6H_5NO) by assigning a somewhat larger error bar of ±0.10 eV. This error will be used in the modeling of the dissociative photoionization of the C_6H_5NO.

Figure 4 shows representative TOF distributions of the parent fragment ions of $C_6H_5NO^+$ at various photon energies, corrected for contamination from ionization events that generated energetic electrons. The parent peak ($C_6H_5NO^+$) is observed at 24.0 μs. The shoulder at slightly longer times of flight, observed in the TOF distribution at 10.58 eV, is due to the ^{13}C isotope peak. The rapidly dissociated fragment ions have a TOF of 20.32 μs. Fragment ions generated in the first acceleration region from slowly dissociating parent ions show up as asymmetric daughter ion time-of-flight distributions, as shown in the data for the top three TOF distributions in Figure 4. If the parent ion lives sufficiently long to enter the first drift region, it will produce a fragment ion that has the same velocity, but a lighter mass, and

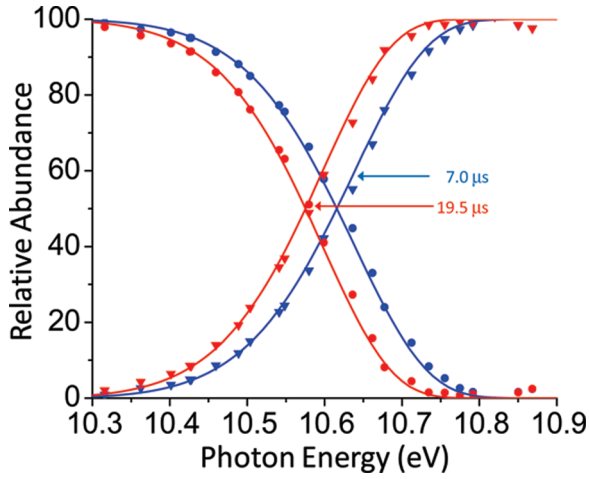

Figure 5. Breakdown diagram for nitrosobenzene. The points represent the experimental relative abundances of the parent (circles) and fragment (triangles) ions at each photon energy. The lines are the simulated results generated by a single SSACM $k(E)$ curve. The two breakdown diagrams differ in how the fragment ions formed in the 25 cm long drift region (drift peak in Figure 4) are treated. In the 7.0 μs data the drift peak is added to the parent peak area, whereas in the 19.5 μs data the drift peak is added to the daughter ion peak area.

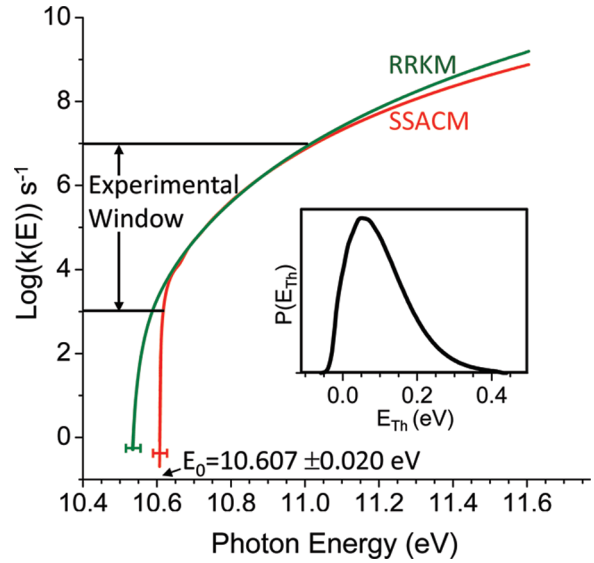

Figure 6. RRKM (green) and SSACM (red) rate curves and ion internal energy distribution (convoluted with both the monochromator resolution and the electron energy analyzer resolution) used to fit the experimental data. The arrow indicates the location of the E_0 determined by SSACM, which is in good agreement with the ATcT value of 10.610 eV. The error bars represent uncertainties in the extrapolated onset by SSACM and RRKM.

thus less kinetic energy. These daughter ions are separated from their parent ions by slowing them down in the last 10 cm. Their reduced translational energy causes them to be slowed down more than the parent ions and results in the daughter ion peak at 24.5 μs. By analyzing the whole TOF distribution, it is possible to derive a dissociation rate constant, which can be measured in the range between 10^3 and 10^7 s^{-1}.

Figure 5 shows the relative abundances (breakdown diagram) of the fragment and parent peaks from 10.3 to 10.9 eV. The $C_6H_5NO^+$ intensity remains zero at photon energies greater than 10.8 eV. Two breakdown diagrams are plotted in Figure 5. The red symbols and the modeled line are plotted by considering the peak at 24.5 μs to be a fragment ion, while the blue symbols and the modeled line are plotted by considering this peak to be part of the parent ion peak. These two diagrams are associated with ions dissociating within 19.5 and 7.0 μs, respectively. A single $k(E)$ curve, shown in Figure 6, is used to model both breakdown diagrams.

Modeling of the TOF Distributions and the Breakdown Diagrams. The experimental data are modeled using experimental parameters and either RRKM or SSACM. For both RRKM and SSACM, the vibrational frequencies of the ion were used to determine density of states, $\rho(E)$. For the RRKM treatment, the vibrational frequencies of the ion equilibrium geometry were used for transition state frequencies less the C−N stretching mode. In addition to the E_0, the four vibrational frequencies corresponding to the transitional modes were scaled to fit the data. For SSACM, the product vibrational frequencies and rotational constants are used to determine the phase space theory transition state. The rotational contribution to the transition state sum of states is scaled by an energy dependent rigidity factor, $f(E)$:

$$f(E) = \exp-\left(\frac{E - E_0}{c}\right) \quad (1)$$

The variable c, which is related to the anisotropy of the interaction potential between the leaving neutral and fragment ion, was optimized to fit the data. The time-of-flight distributions in Figure 4 and breakdown curves in Figure 5 are modeled by taking into account the thermal energy distribution of the room temperature sample. The solid lines through the data points is the best fit using the $k(E)$ curve shown in Figure 6. Figure 6 also shows the calculated ion internal energy distribution for a single photon energy, which is obtained by assuming that the neutral thermal energy distribution is transposed to the ionic manifold. Because the ion internal energy distribution covers nearly the entire experimental window, it is impossible to obtain accurate $k(E)$ information without accounting for the ion internal energy distribution. This is done by calculating TOF distributions at each ion internal energy and combining them, weighted by the ion internal energy distribution. The RRKM and SSACM rate curves are essentially identical throughout the experimental window but diverge at both higher and lower energies. At lower energies, the SSACM transition state is at the phase space limit, and therefore, the $k(E)$ curve has a much stronger energy dependence than does the RRKM rate curve, so that SSACM predicts a higher E_0 than RRKM. The extrapolated E_0s are 10.533 ± 0.020 and 10.607 ± 0.020 eV for RRKM and SSACM, respectively. For both rate models, the somewhat large uncertainty in IE(C_6H_5NO) was taken into account when computing the uncertainties in the E_0s. However, because the ionic dissociation energy (E_0−IE(C_6H_5NO)) changes to offset changes in the IE(C_6H_5NO), this had a nearly negligible effect on the uncertainty in E_0. SSACM fits to the data were obtained with a fitting parameter c of 100 meV. For RRKM, fits were obtained by scaling the transitional frequencies by 0.12, indicating a very loose transition state with an entropy of activation of 66 J mol^{-1} K^{-1}. Although good agreement between the two models is observed within the experimental window, they extrapolate to different E_0s. Previous studies have shown that the RRKM model extrapolates to E_0 values that are too low, so we utilize the SSACM results for extracting thermochemical information.[40]

Auxiliary Thermochemical Values. Several auxiliary thermochemical quantities are needed in the ensuing discussion of the experimental result. Namely, using E_0 to obtain the absolute

thermochemistry of the constituents of the cycle in Figure 1 via a traditional sequential (i.e., non-ATcT) approach requires a species (or process) with known thermochemistry for calibration. Obviously, the uncertainty in the latter will copropagate to any derived thermochemistry. Even if one sets aside the problem of inconsistency between the literature values for $\Delta_f H°_0(C_6H_5^+)$ given in Table 1, their uncertainties are too large (± 4 kJ mol^{-1} for the *nominally* most accurate value) to meaningfully improve the thermochemistry of this cycle by measuring E_0. In addition to furnishing significantly more accurate enthalpies of formation of both $C_6H_5^+$ and C_6H_5, ATcT also provides an accurate value for $\Delta_f H°_0$(NO) of 90.59 $\pm$ 0.07 kJ mol^{-1} (see also Ruscic et al.;[46] note that the widely used enthalpy of formation of NO from the JANAF Tables[130] is wrong, as opposed to the value from Gurvich et al.,[131] which is less precise but intrinsically more accurate).

The remaining thermochemical quantity of interest in the present context is the bond dissociation energy of nitrosobenzene. As mentioned before, the value reported by Park et al.[3] (226.8 $\pm$ 2.1 kJ/mol at 0 K) from measurements of kinetic rate constants for the forward[3] and reverse[4] processes coupled to their modeling of the pressure falloff looks sufficiently accurate for the current purpose. However, that value appears discordant with the values reported by Horn et al.[5] and Choo et al.[6] Horn et al.[5] also determined the forward and reverse rate constants and obtained a 0 K value of 209 kJ mol^{-1} (50 kcal mol^{-1}, no explicit uncertainty given). Choo et al.,[6] by combining their measured forward rate constant with an estimated rate constant for the reverse process, inferred a 298 K bond dissociation enthalpy of 215.5 $\pm$ 4.2 kJ mol^{-1} (51.5 $\pm$ 1 kcal mol^{-1}), corresponding to 211 kJ mol^{-1} at 0 K. Thus, the two values of Horn et al. and Choo et al. appear to mutually agree (differing only by 2 kJ/mol), and both are significantly lower (by >15 kJ mol^{-1}) than the value of Park et al. In order to shed light on the apparent discrepancies, a slightly more elaborate scrutiny of all three values is necessary.

Though Horn et al.[5] did not explicitly provide an uncertainty for their bond dissociation energy, they do provide uncertainties for the determined rate constants for the forward and reverse processes. From a second law treatment of the resulting equilibrium constant, we obtain a dissociation enthalpy of 211 kJ mol^{-1} at 810 K; with our partition function for nitrosobenzene (RRHO, except for the torsional contribution[132]), this indeed reduces at 0 K to 210 kJ mol^{-1} (50.$_2$ kcal mol^{-1}, cf. to 50 kcal/mol as given by Horn et al.), but the associated uncertainty (based on propagating 2σ uncertainties of the rate constants) is quite large, $\pm$ 18 kJ mol^{-1}, and thus, in fact, the result of Horn et al. overlaps with the value of Park et al. The third law treatment of the same rate constants produces a Gibbs energy of 89 kJ mol^{-1} at 810 K, which reduces to 220 kJ mol^{-1} at 0 K, a value that is somewhat closer to the result of Park et al., but at the expense of an even larger nominal uncertainty, $\pm$30 kJ mol.$^{-1}$ (One needs to note, though, that the latter uncertainty is likely to be overestimated, because the A factor and E_0 in a fitted Arrhenius expression are typically very strongly correlated and hence the corresponding covariance matrix–which is virtually never given–has substantial off-diagonal elements.)

The older dissociation enthalpy of Choo et al.[6] is based on the measured rate for the forward reaction and the assumption that the reverse activation barrier is approximately 0. Such an assumption is, in fact, quite reasonable: both Park et al. and Horn et al. have small negative activation energies in the expression for the reverse rate constant. Thus, the second law bond dissociation enthalpy deduced from the forward rate constant of Choo et al. amounts to 211 kJ mol^{-1} at 700 K, corresponding to 209 kJ mol^{-1} at 0 K. Choo et al., however, obtain a slightly higher bond dissociation enthalpy by combining the measured forward rate constant with a guesstimate for the reverse rate constant to create a "virtual" third law Gibbs energy, which is then combined with a guesstimate for the reaction entropy to obtain the bond enthalpy. The uncertainty proposed by Choo et al. is $\pm$4 kJ mol^{-1}, based essentially on their estimate of the possible error in the guesstimated reaction entropy. The error in the latter is, in fact, at least twice as large as they assumed, and is clearly not the only source of error that needs to be considered. Taking into account also the fact that their guesstimated reverse rate constant appears to be off by several orders of magnitude suggests to us that a better estimate of the uncertainty of the bond dissociation enthalpy of Choo et al. would be of the order of $\pm$20 kJ mol^{-1}.

The above analysis suggests that, within their (substantial) uncertainties, the bond dissociation energies of Horn et al.[5] and Choo et al.[6] do not disagree with the more accurate value given by Park et al.[3] Thus, rather than there being an essential discord between the existing bond dissociation energies of nitrosobenzene, the discerning question becomes whether the significantly tighter uncertainty proposed by Park et al. is realistic. Unfortunately, Park et al. do not state clearly whether their uncertainty indeed corresponds to the expected 95% confidence interval, nor do they give a detailed genesis of their error bar that might allow a more rigorous analysis. The listed uncertainty ($\pm$0.5 kcal/mol) appears to be related by approximately a factor of 2 to the 1σ ($\pm$0.22 kcal/mol) that describes the dispersion of the central third law values at individual experimental temperatures (each reduced to D_0 by using their partition function). This dispersion, however, describes only the precision and does not include an estimate of potential systematic uncertainties of the individual third law values; on the other hand, a more appropriate quantity related to precision would be the dispersion of the mean, which is in this particular case 3 times lower. Another approach to get a handle on the estimate of the uncertainty in the bond dissociation enthalpy is to propagate the uncertainties given in the Arrhenius expressions for the kinetic rate constants. Assuming that these uncertainties are 2σ (which seems to be the case for the reverse rate constant obtained by the same group in an earlier paper,[4] though, without repeating their modeling of the pressure falloff, it is not completely clear if it also pertains to the forward rate constant,[3] which happens to be the leading source of the uncertainty in the resulting BDE), our treatment using the third law approach produces a bond dissociation Gibbs energy of 139.9 $\pm$ 4.6 kJ mol^{-1} at 525 K (which is the middle of the temperature gap between the ranges of validity of the forward and reverse rate constants), while the application of the second law produces an enthalpy of 238.3 $\pm$ 9.2 kJ mol^{-1}. Using our partition functions, these enthalpies reduce to 223.7 $\pm$ 4.6 and 234.8 $\pm$ 9.2 kJ mol^{-1}, respectively, at 0 K. Park et al., however, have in their treatment applied the third law approach to the actually measured individual rate constants for the reverse process, which were coupled to the rate constants of the forward process extrapolated to lower temperatures. An analogous treatment by second law would produce a bond dissociation enthalpy of 235.8 $\pm$ 10.0 kJ mol^{-1} at 382 K, which would convert to 231.6 $\pm$ 10.0 kJ/mol at 0 K. Since the averaging procedure used by Park et al. to derive their recommended value for $D_0(C_6H_5-NO)$ should tend to produce a lower uncertainty than those associated with individual third and second law values, the above, in fact, does not unequivocally rule out the proposed uncertainty of Park et al. as being overly

optimistic, although there seems to be some room for suspecting that it may, in fact, be representing only 1σ. Keeping in mind the latter possibility, we take the pragmatic approach in which, for the purpose of the discussion that will examine the potential ramifications of the experimental data by using the traditional (non-ATcT) approach, we make a leap of faith and use *as a working hypothesis* the assumption that the uncertainty of the dissociation energy of nitrosobenzene as given by Park et al.[3] is correct. This working hypothesis, however, will not bias in any manner the final ATcT analysis. There, the determinations of Park et al.,[3] Horn et al.,[5] and Choo et al.[6] will be added to the thermochemical network in the form of actual second and third law analysis values and will be subjected to the ATcT statistical analysis that evaluates the consistency of every determination against the cumulative knowledge of the thermochemical network and, if and when necessary, iteratively readjusts any and all uncertainties that appear to be "optimistic".[1,2]

Direct Ramifications of the Experimental $E_0(C_6H_5^+/C_6H_5NO)$. The experimentally determined E_0 (10.607 ± 0.020 eV), when paired up with the value $D_0(C_6H_5NO) = 226.8 \pm 2.1$ kJ mol^{-1} of Park et al.,[3] produces IE(C_6H_5) = 8.257 ± 0.030 eV, in excellent agreement with the initial ATcT value of 8.274 ± 0.011 eV given earlier and with the computed value of 8.261 ± 0.035 by Lau and Ng[38] and in satisfactory agreement with the experimental feature at 8.32 ± 0.04 eV observed by Butcher et al.[8] If E_0 were to be paired with the C_6H_5-NO dissociation energy of Horn et al.,[5] the resulting IE of phenyl would be higher, 8.44 eV, though with a significantly larger uncertainty (estimated to be ±0.20 eV). Using the dissociation energy of Choo et al.[6] would lead to a similarly high IE of 8.42 eV. In the latter case, accepting the original uncertainty would produce a rather tight nominal uncertainty of ±0.05 eV that would make this result incongruent with the remaining knowledge, but as discussed above, a more realistic analysis suggests a more relaxed uncertainty of ±0.22 eV.

Our measured E_0 also provides access to a $\Delta_f H°(C_6H_5NO)$, providing that the enthalpies of formation of $C_6H_5^+$ and NO are known. Using the ATcT values given above produces a $\Delta_f H°_0(C_6H_5NO)$ of 216.0 ± 2.2 kJ mol^{-1}. This value is in good agreement with the 0 K enthalpy of formation of C_6H_5NO of 214.4 ± 2.2 kJ mol^{-1} that can be derived from the ATcT heats of formation of C_6H_5 and NO and the homolytic bond dissociation energy of C_6H_5NO of Park et al.[3] Curiously, the 298 K value of 201.3 ± 4.2 kJ mol^{-1} (48.1 ± 1 kcal mol^{-1}) for $\Delta_f H°(C_6H_5NO)$ given explicitly by Choo et al.[6] (and currently listed by the NIST WebBook[133] as the only available enthalpy of formation of nitrosobenzene), which converts to 218.4 ± 4.2 kJ mol^{-1} at 0 K, fortuitously agrees with the above value(s) within the given uncertainties because of cancellation of errors: its essential foundation is a combination of a low value for the enthalpy of formation of phenyl (326 kJ mol^{-1}, i.e. 78 kcal/mol) with a bond dissociation enthalpy of C_6H_5-NO that the present analysis suggests as being too low by nearly four times its originally declared uncertainty of ±4 kJ mol^{-1}. The $\Delta_f H°_0(C_6H_5NO)$ values obtained by combining the bond dissociation enthalpies of Choo et al.[6] and Horn et al.[5] with the ATcT values for phenyl and NO would be 230 ± 20 and 232 ± 18 kJ mol^{-1}, respectively (and the corresponding 298 K values would be 17 kJ mol^{-1} lower).

Final ATcT Thermochemical Values. The above discussion suggests that the currently determined $E_0(C_6H_5^+/C_6H_5NO)$ as well as prior determinations[3,5,6] of the homolytic C−H bond dissociation of C_6H_5NO are all both mutually consistent (within their respective uncertainties) and consistent with the initial ATcT results. Thus, other than producing a value for the enthalpy of formation of nitrosobenzene that is more accurate than what could be obtained by sequential thermochemistry from any single determination, the introduction of the additional knowledge relating to C_6H_5NO into C(A)TN should be rather uneventful; i.e., it should cause only minor changes in the enthalpies of formation of the other species involved. That is indeed the case.

Table 2 lists the targeted thermochemical values obtained by the ATcT approach, based on the augmented C(A)TN ver. 1.110. The resulting enthalpy of formation of nitrosobenzene is $\Delta_f H°_{298}(C_6H_5NO) = 198.6 \pm 1.5$ kJ mol^{-1} (215.6 kJ mol^{-1} at 0 K). The current ATcT enthalpies of formation of phenyl, phenylium, and phenide (for the ions, given in the stationary electron convention, such as that used by the tables of Lias et al.[134]) are $\Delta_f H°_{298}(C_6H_5) = 337.3 \pm 0.6$ kJ mol^{-1} (350.6 kJ mol^{-1} at 0 K), $\Delta_f H°_{298}(C_6H_5^+) = 1136.8 \pm 1.0$ kJ mol^{-1} (1148.7 kJ mol^{-1} at 0 K), and $\Delta_f H°_{298}(C_6H_5^-) = 232.0 \pm 0.5$ kJ mol^{-1} (244.9 kJ mol^{-1} at 0 K).

The corresponding value for the adiabatic ionization energy of phenyl is 8.272 ± 0.010 eV. This result strongly suggests that the 8.32 eV photoelectron feature reported by Butcher et al.[8] indeed corresponds to the unresolved rotational envelope of the $0 \leftarrow 0$ vibrational transition from the ground state X $^2A_1$ of phenyl to the ground state X $^1A_1$ of phenylium.[135] The ATcT value for the electron affinity of phenyl is 1.095 ± 0.005 eV, nearly identical to the experimental value 1.096 ± 0.006 eV of Gunion et al.[63]

The enthalpies of formation of phenyl and of benzene, together with the C−H bond dissociation enthalpy of benzene, constitute a tightly related trio of thermochemical quantities. The current ATcT value for the enthalpy of formation of gas-phase benzene at 298.15 K, 83.2 ± 0.3 kJ mol^{-1} (or 100.7 kJ mol^{-1} at 0 K), refines the older and less accurate values selected in the popular evaluation by Cox and Pilcher,[136] $82.8_9 \pm 0.5_4$ kJ mol^{-1} (19.81 ± 0.13 kcal mol^{-1}), and its successors, by Pedley et al.[137] and Pedley,[138] which list the 298.15 K value at 82.6 ± 0.7 kJ mol^{-1}, as well as the more recent reevaluation of Roux et al.[139] (82.9 ± 0.9 kJ mol^{-1}). The current ATcT value of the bond dissociation energy of benzene is $D_0(C_6H_5-H) = 465.9 \pm 0.6$ kJ mol^{-1} (111.35 ± 0.13 kcal mol^{-1}) or $BDE_{298}(C_6H_5-H) = 472.1 \pm 0.6$ kJ mol^{-1} (112.83 ± 0.13 kcal mol^{-1}) and represents the most accurate value for this important quantity available so far. Of the numerous experimental literature values for this quantity that are available, the one that requires highlighting is the 298.15 K value of 472.2 ± 2.2 kJ mol^{-1} (112.9 ± 0.6 kcal mol^{-1}) given by Ervin and DeTuri[12] (see also Blanksby and Ellison[13]). Davico et al.[17] have originally derived a 300 K BDE of 113.5 ± 0.5 kcal mol^{-1} by combining the electron affinity of phenyl determined by Gunion et al.[63] with their own determination of the gas-phase acidity of benzene. The latter was based on their measurement of the relative gas-phase acidity of benzene, coupled to the then-prevailing value for the gas-phase acidity of ammonia; Ervin and DeTuri[12] improved on this negative ion cycle by introducing a better value for the gas-phase acidity of ammonia. (Parenthetically, the ATcT TN does not include the bond dissociation enthalpy of benzene of Ervin and Deturi,[12] which is a derived quantity; rather, it contains, inter alia, the relative gas-phase acidity measurement of Davico et al.[17] and electron affinity measurement of Gunion et al.[63]) On the theoretical side, the W3.2lite 0 K result of 111.02 (±0.40) kcal mol^{-1} (464.5 kJ mol^{-1}) and the slightly less expensive W2.2 result of 111.48 kcal mol^{-1} (466.4 kcal mol^{-1}), both reported by Karton et al.,[128] appear to be the closest to the

TABLE 2: Current ATcT Thermochemical Values[a]

quantity	0 K	298.15 K	uncertainty	units	quantity	0 K	298.15 K	uncertainty	units
$\Delta_f H°(C_6H_5)$[b]	350.6	337.3	±0.6	kJ mol^{-1}	$\Delta_{acid}G°(C_6H_6)$[k]	1672.3	1641.4	±0.4	kJ mol^{-1}
$\Delta_f H°(C_6H_5^+)$[b]	1148.7	1136.8	±1.0	kJ mol^{-1}	$\Delta_{deprot}H°(C_6H_6)$[l]	ditto	1678.8	±0.4	kJ mol^{-1}
$\Delta_f H°(C_6H_5^-)$[b]	244.9	232.0	±0.5	kJ mol^{-1}	$IE(C_6H_5F)$[h]	9.2032	−	±0.0004	eV
$\Delta_f H°(C_6H_6)$[b]	100.7	83.2	±0.3	kJ mol^{-1}	$IE(C_6H_5Cl)$[h]	9.0723	−	±0.0004	eV
$\Delta_f H°(C_6H_6^+)$[b]	992.6	976.1	±0.3	kJ mol^{-1}	$IE(C_6H_5Br)$[h]	8.9974	−	±0.0006	eV
$\Delta_f H°(C_6H_5NO)$[b]	215.6	198.6	±1.5	kJ mol^{-1}	$IE(C_6H_5I)$[h]	8.7578	−	±0.0006	eV
$\Delta_f H°(C_6H_5F)$[b]	−99.7	−115.4	±1.0	kJ mol^{-1}	$BDE(C_6H_5-NO)$[m]	225.6	229.7	±1.4	kJ mol^{-1}
$\Delta_f H°(C_6H_5F^+)$[b]	788.3	773.6	±1.0	kJ mol^{-1}	$BDE(C_6H_5-F)$[m]	527.5	532.0	±1.2	kJ mol^{-1}
$\Delta_f H°(C_6H_5Cl)$[b]	67.2	52.2	±0.6	kJ mol^{-1}	$BDE(C_6H_5-Cl)$[m]	403.0	406.4	±0.8	kJ mol^{-1}
$\Delta_f H°(C_6H_5Cl^+)$[b]	942.5	928.6	±0.6	kJ mol^{-1}	$BDE(C_6H_5-Br)$[m]	341.5	344.2	±1.3	kJ mol^{-1}
$\Delta_f H°(C_6H_5Br)$[b]	127.0	104.9	±1.3	kJ mol^{-1}	$BDE(C_6H_5-I)$[m]	279.9	282.2	±1.1	kJ mol^{-1}
$\Delta_f H°(C_6H_5Br^+)$[b]	995.1	973.8	±1.3	kJ mol^{-1}	$E_0(C_6H_5^+/C_6H_5NO)$[n,o]	10.610	−	±0.015	eV
$\Delta_f H°(C_6H_5I)$[b]	177.9	161.9	±1.0	kJ mol^{-1}	$E_0(C_6H_5^+/C_6H_6)$[n]	13.101	−	±0.010	eV
$\Delta_f H°(C_6H_5I^+)$[b]	1022.8	1007.4	±1.0	kJ mol^{-1}	$E_0(C_6H_5^+/C_6H_5F)$[n]	13.740	−	±0.014	eV
$\Delta_f H°(C_6H_6)$ (liquid)[b]	−	49.2	±0.3	kJ mol^{-1}	$E_0(C_6H_5^+/C_6H_5Cl)$[n]	12.449	−	±0.011	eV
$\Delta_f H°(C_6H_5F)$ (liquid)[b]	−	−150.0	±1.0	kJ mol^{-1}	$E_0(C_6H_5^+/C_6H_5Br)$[n]	11.812	−	±0.012	eV
$\Delta_f H°(C_6H_5Cl)$ (liquid)[b]	−	11.3	±0.6	kJ mol^{-1}	$E_0(C_6H_5^+/C_6H_5I)$[n]	11.173	−	±0.008	eV
$\Delta_f H°(C_6H_5Br)$ (liquid)[b]	−	60.2	±1.3	kJ mol^{-1}	$TAE_0(C_6H_5)$[p]	4997.9	−	±0.7	kJ mol^{-1}
$\Delta_f H°(C_6H_5I)$ (liquid)[b]	−	113.1	±1.1	kJ mol^{-1}	$TAE_0(C_6H_5^+)$[p]	4199.7	−	±1.0	kJ mol^{-1}
$\Delta_f H°(NO)$[b,c,d]	90.59	91.09	±0.07	kJ mol^{-1}	$TAE_0(C_6H_5^-)$[p]	5103.6	−	±0.6	kJ mol^{-1}
$\Delta_f H°(C)$[b,c,e]	711.38	716.87	±0.06	kJ mol^{-1}	$TAE_0(C_6H_6)$[p]	5463.8	−	±0.4	kJ mol^{-1}
$\Delta_f H°(N)$[b,c,e]	470.57	472.44	±0.03	kJ mol^{-1}	$TAE_0(C_6H_6^+)$[p]	4571.9	−	±0.4	kJ mol^{-1}
$\Delta_f H°(O)$[b,c,f]	246.844	249.229	±0.002	kJ mol^{-1}	$TAE_0(C_6H_5NO)$[p]	5850.3	−	±1.5	kJ mol^{-1}
$\Delta_f H°(H)$[b,c,f]	216.034	217.998	±0.000	kJ mol^{-1}	$TAE_0(C_6H_5F)$[p]	5525.5	−	±1.1	kJ mol^{-1}
$\Delta_f H°(F)$[b,c,g]	77.26	79.37	±0.06	kJ mol^{-1}	$TAE_0(C_6H_5F^+)$[p]	4637.5	−	±1.1	kJ mol^{-1}
$\Delta_f H°(Cl)$[b,c,f]	119.621	121.302	±0.002	kJ mol^{-1}	$TAE_0(C_6H_5Cl)$[p]	5400.9	−	±0.7	kJ mol^{-1}
$\Delta_f H°(Br)$[b,c]	117.92	111.85	±0.06	kJ mol^{-1}	$TAE_0(C_6H_5Cl^+)$[p]	4525.6	−	±0.7	kJ mol^{-1}
$\Delta_f H°(I)$[b,c]	107.157	106.757	±0.002	kJ mol^{-1}	$TAE_0(C_6H_5Br)$[p]	5339.4	−	±1.3	kJ mol^{-1}
$IE(C_6H_5)$[h]	8.272	−	±0.010	eV	$TAE_0(C_6H_5Br^+)$[p]	4471.3	−	±1.3	kJ mol^{-1}
$EA(C_6H_5)$[i]	1.095	−	±0.005	eV	$TAE_0(C_6H_5I)$[p]	5277.8	−	±1.1	kJ mol^{-1}
$IE(C_6H_6)$[h]	9.24373	−	±0.00004	eV	$TAE_0(C_6H_5I^+)$[p]	4432.8	−	±1.1	kJ mol^{-1}
$BDE(C_6H_5-H)$[j]	465.9	472.1	±0.6	kJ mol^{-1}					

[a] All values are from C(A)TN ver. 1.110. Unless noted otherwise, all species are gaseous. [b] Enthalpy of formation; for ions it is given here in the "stationary electron" convention (as used, for example, in the tables of Lias et al.[145]) and can be converted to the "thermal electron" convention (used, for example, in the JANAF Tables[130] or the Russian Tables[131]) by simply adding 2.5*RT* (6.197 kJ mol^{-1} at 298.15 K) to the listed value for the cation or subtracting the same amount from the listed value for the anion. [c] Auxiliary value, listed here for completeness. [d] Current ATcT value, essentially unchanged (within the round off error) from the previously published ATcT value; see Ruscic et al.[46] [e] Current ATcT value, which supersedes earlier interim ATcT values disseminated by private communication(s); the full genesis of this value will be the topic of a separate publication. [f] Current ATcT value, unchanged from the previously published ATcT value: see Ruscic et al.[1] [g] Current ATcT value, improved from the previously published ATcT value; see Ruscic et al.[1] [h] Adiabatic ionization energy, $C_6H_5X \rightarrow C_6H_5X^+ + e^-$, X = nil, H, F, Cl, Br, I. [i] Adiabatic electron affinity of phenyl, $C_6H_5^- \rightarrow C_6H_5 + e^-$. [j] C−H bond dissociation enthalpy of benzene, $C_6H_6 \rightarrow C_6H_5 + H$, at 0 K identical to $D_0(C_6H_5-H)$. [k] Gas phase acidity of benzene; Gibbs energy of $C_6H_6 \rightarrow C_6H_5^- + H^+$. [l] Enthalpy of deprotonation of benzene, enthalpy of $C_6H_6 \rightarrow C_6H_5^- + H^+$. [m] C−X bond dissociation enthalpy $C_6H_5X \rightarrow C_6H_5 + X$, at 0 K identical to $D_0(C_6H_5-X)$. [n] Appearance energy of phenylium from C_6H_5X, $C_6H_5X \rightarrow C_6H_5^+ + X + e^-$. [o] The direct experimental value of $E_0(C_6H_5^+/C_6H_5NO)$ obtained in this study is 10.607 ± 0.020 eV. [p] Total atomization energy into neutral atoms (even if the species is an ion); the related gas-phase enthalpies of formation of the atoms are also given in this table.

current ATcT bond dissociation energy. As already mentioned, a number of popular composite electronic structure methods are based on unrestricted wave functions and suffer from severe spin contamination problems when describing phenyl. As a result, they have a propensity toward producing a systematically high value for the BDE of benzene (for example, recent G3X calculations[140] have resulted in suggesting a 298 K bond dissociation energy of 114.0 kcal mol^{-1}).

Also listed in Table 2 are several related thermochemical quantities derived from the same version of C(A)TN, such as the enthalpies of formation of monohalobenzenes. In traditional thermochemical tabulations,[136−138] the recommended enthalpies of formation of monohalobenzenes (as well as benzene itself) rely nearly entirely on condensed-phase calorimetric determinations, combined with the respective enthalpies of vaporization. As opposed to this, the values given in Table 2 (particularly for the heavier halobenzenes) are the result of balancing the available condensed-phase thermochemistry with the newer gas-phase thermochemically relevant determinations, such as the dissociative photoionization onsets of the type $C_6H_5X + h\nu \rightarrow C_6H_5^+ + X$ determined by Stevens et al.[40] Thus, for example, Cox and Pilcher[136] give $\Delta_f H°_{298}(C_6H_5I) = 163.6 \pm 5.4$ kJ mol^{-1} (39.1 ± 1.3 kcal mol^{-1}), while Pedley et al.[137] subsequently revised this quantity slightly upward to 164.9 ± 5.9 kJ mol^{-1}. The value of Pedley et al. relies entirely on combustion calorimetry of liquid iodobenzene measured by Smith,[141] combined with an estimated[136] vaporization enthalpy to arrive at the gas-phase species. Cox and Pilcher[136] have, in addition, considered the condensed-phase calorimetric data of Hartley et al.[142] (bromination and iodination of diphenyl mercury) in combination with the calorimetric data of Chernick et al.[143] (hydrochlorination of diphenyl mercury in benzene solution). Though still contained within the uncertainty envelopes of the earlier values of Cox and Pilcher,[136] Pedley et al.,[137] and Pedley,[138] the current ATcT value of 161.9 ± 1.0 kJ mol^{-1} is significantly more accurate. In addition to reproducing in a satisfactory manner the available calorimetric determinations, the ATcT value for iodobenzene produces, for example, $D_0(C_6H_5-I) = 279.9 \pm 1.1$ kJ mol^{-1}. The latter is in excellent agreement with the 0 K BDEs of 279.1 ± 4.2 kJ mol^{-1} (66.7 ± 1.0 kcal mol^{-1}) of Kumaran et al.,[144] and 279 ± 5 kJ mol^{-1} of Heckmann et al.[14] (converted from their 298.15 K value of 282 mol^{-1}). At the same time, the ATcT value for iodobenzene produces $E_0(C_6H_5^+/C_6H_5I) = 11.173 \pm 0.008$ eV, which is in excellent agreement with the experimental values $E_0(C_6H_5^+/C_6H_5I) = 11.173^{+0.020}/_{-0.027}$ eV (SSACM) and $11.178^{+0.010}/_{-0.011}$ eV (VTST) obtained recently by Stevens et al.[40] Mutatis mutandis, one can make similar statements about the other ATcT values for

monohalobenzenes, with the exception of fluorobenzene, for which currently there are no satisfactory experimental determinations of either the BDE or photodissociative ionization onsets.

Finally, Table 2 includes the 0 K total atomization energies, TAE_0, for the target species. These quantities may prove useful to developers and practitioners of state-of-the-art electronic structure methods. For the sake of completeness, Table 2 also includes current ATcT values for the gas-phase enthalpies of formation of the constituent atoms. These are of particular interest to computational thermochemistry, since they link computed total atomization energies to practical enthalpies of formation. While work is still in progress on several of these key thermochemical quantities, the current values have been sufficiently stable over several versions of C(A)TN to warrant their release as interim ATcT results. Fully converged values for the enthalpies of formation of atoms, together with a detailed account of their provenance and genesis, will be the topic of a separate report.

Concluding Remarks

The present study combines experimental photoionization measurements and the ATcT approach. The 0 K dissociation onset for nitrosobenzene has been determined by SSACM modeling of data obtained by TPEPICO to be 10.607 ± 0.020 eV. A preliminary analysis of the background kinetic rate determinations suggests that the homolytic BDE of nitrosobenzene obtained by Park et al.[3] is more accurate than the other available determinations of the same quantity. Using the traditional sequential thermochemistry approach and pairing up the photodissociative ionization threshold with the selected measurement of the BDE would suggest an adiabatic IE of phenyl of 8.257 ± 0.030 eV. When ATcT is employed to obtain a completely independent value for the same quantity (without referring to any measurements involving nitrosobenzene), it produces 8.274 ± 0.011 kJ mol^{-1}, thus corroborating both the TPEPICO threshold and the BDE of Park et al. After inclusion of the additional thermochemical knowledge related to nitrosobenzene, ATcT produces a slightly refined value for the IE of phenyl of 8.272 ± 0.010 eV, as well as a number of other related thermochemical quantities of interest (such as the enthalpy of formation of phenyl, the associated C−H BDE of benzene, etc.) that are summarized in Table 2.

Acknowledgment. This work was supported by the U.S. Department of Energy, Office of Basic Energy Sciences, Division of Chemical Sciences, Geosciences and Biosciences under Contract No. DE-AC02-06CH11357 (at Argonne National Laboratory) and DE-FG02-97ER14776 (at UNC−Chapel Hill). We thank Andras Bodi of the Swiss Light Source for help in running the nitrosobenzene TPES. Portions of this research are related to the effort of the Task Group of the International Union of Pure and Applied Chemistry, "Selected Free Radicals and Critical Intermediates: Thermodynamic Properties from Theory and Experiment" (IUPAC Project 2003-024-1-100).

References and Notes

(1) Ruscic, B.; Pinzon, R. E.; Morton, M. L.; Laszevski, G.; Bittner, S. J.; Nijsure, S. G.; Amin, K. A.; Minkoff, M.; Wagner, A. F. *J. Phys. Chem. A* **2004**, *108*, 9979–9997.

(2) Ruscic, B.; Pinzon, R. E.; Morton, M. L.; Laszevski, G.; Bittner, S. J.; Nijsure, S. G.; Amin, K. A.; Minkoff, M.; Leahy, D.; Montoya, D.; Wagner, A. F. *J. Phys. Conf. Ser.* **2005**, *16*, 561–570.

(3) Park, J.; Dyakov, I. V.; Mebel, A. M.; Lin, M. C. *J. Phys. Chem. A* **1997**, *101*, 6043–6047.

(4) Yu, T.; Lin, M. C. *J. Phys. Chem.* **1994**, *98*, 2105–2109.

(5) Horn, C.; Frank, P.; Tranter, R. S.; Schaugg, J.; Grotheer, H.-H.; Just, T. *Proc. Combust. Inst. #26* **1996**, 575–582.

(6) Choo, K. Y.; Golden, D. M.; Benson, S. W. *Int. J. Chem. Kin.* **1975**, *7*, 713–724.

(7) Sergeev, Y. L.; Akopyan, M. E.; Vilesov, F. I.; Kleimenov, V. I. *Opt. Spect.* **1972**, *32*, 230–231.

(8) Butcher, V.; Costa, M. L.; Dyke, J. M.; Ellis, A. R.; Morris, A. *Chem. Phys.* **1987**, *115*, 261–267.

(9) Alecu, I. M.; Gao, Y.; Hsieh, P.-C.; Sand, J. P.; Ors, A.; McLeod, A.; Marshall, P. *J. Phys. Chem. A* **2007**, *111*, 3970–3976.

(10) Sivaramakrishnan, R.; Tranter, R. S.; Brezinsky, K. *J. Phys. Chem. A* **2006**, *110*, 9388–9399.

(11) Sivaramakrishnan, R.; Tranter, R. S.; Brezinsky, K. *J. Phys. Chem. A* **2006**, *110*, 9400–9404.

(12) Ervin, K. M.; DeTuri, V. F. *J. Phys. Chem. A* **2002**, *106*, 9947–9956.

(13) Blanksby, S. J.; Ellison, G. B. *Acc. Chem. Res.* **2003**, *36*, 255–263.

(14) Heckmann, E.; Hippler, H.; Troe, J. *Proc. Combust. Inst.* **1996**, *26*, 543–550.

(15) Tsang, W. Heats of Formation of Organic Free Radicals by Kinetic Methods. In *Energetics of Organic Free Radicals*; Martinho Simões, J. A., Greenberg, A., Liebman, J. F., Eds.; Chapman & Hall: London, 1996; pp 22−58.

(16) Robaugh, D.; Tsang, W. *J. Phys. Chem.* **1986**, *90*, 5363–5367.

(17) Davico, G. E.; Bierbaum, V. M.; DePuy, C. H.; Ellison, G. B.; Squires, R. R. *J. Am. Chem. Soc.* **1995**, *117*, 2590–2599.

(18) Berkowitz, J.; Ellison, G. B.; Gutman, D. *J. Phys. Chem.* **1994**, *98*, 2744–2765.

(19) Kiefer, J. H.; Mizerka, L. J.; Patel, M. R.; Wei, H. C. *J. Phys. Chem.* **1985**, *89*, 2013–2019.

(20) McMillen, D. F.; Golden, D. M. *Annu. Rev. Phys. Chem.* **1982**, *33*, 493–532.

(21) Rosenstock, H. M.; Stockbauer, R.; Parr, A. C. *J. Chem. Phys.* **1980**, *73*, 773–777.

(22) Chamberlain, G. A.; Whittle, E. *Trans. Faraday Soc.* **1971**, *67*, 2077–2084.

(23) Egger, K. W.; Cocks, A. T. *Helv. Chim. Acta* **1973**, *56*, 1516–1536.

(24) Golden, D. M.; Benson, S. W. *Chem. Rev.* **1969**, *69*, 125–134.

(25) Rodgers, A. S.; Golden, D. M.; Benson, S. W. *J. Am. Chem. Soc.* **1967**, *89*, 4578–4583.

(26) Ripoche, X.; Dimicoli, I.; Botter, R. *Int. J. Mass Spectrom. Ion. Proc.* **1991**, *107*, 165–182.

(27) Lifshitz, C.; Louage, F.; Aviyente, V.; Song, K. *J. Phys. Chem.* **1991**, *95*, 9298–9302.

(28) Malinovich, Y.; Lifshitz, C. *J. Phys. Chem.* **1986**, *90*, 2200–2203.

(29) Dannacher, J.; Rosenstock, H. M.; Buff, R.; Parr, A. C.; Stockbauer, R.; Bombach, R.; Stadelmann, J. P. *Chem. Phys.* **1983**, *75*, 23–35.

(30) Malinovich, Y.; Arakawa, R.; Haase, G.; Lifshitz, C. *J. Phys. Chem.* **1985**, *89*, 2253–2260.

(31) Dunbar, R. C. *Chem. Phys. Lett.* **1985**, *115*, 349–352.

(32) Dunbar, R. C.; Honovich, J. P. *Int. J. Mass Spectrom. Ion. Proc.* **1984**, *58*, 25–41.

(33) Rosenstock, H. M.; Stockbauer, R.; Parr, A. C. *J. Chem. Phys.* **1979**, *71*, 3708–3714.

(34) Pratt, S. T.; Chupka, W. A. *Chem. Phys.* **1981**, *62*, 153–163.

(35) Beauchamp, J. L. *Adv. Mass Spectrom.* **1974**, *6*, 717–723.

(36) Hrusak, J.; Schröder, D.; Iwata, S. *J. Chem. Phys.* **1997**, *106*, 7541–7549.

(37) Nicolaides, A.; Smith, D. M.; Jensen, F.; Radom, L. *J. Am. Chem. Soc.* **1997**, *119*, 8083–8088.

(38) Lau, K.-C.; Ng, C. Y. *J. Chem. Phys.* **2006**, *124*, 044323/1-044323/9.

(39) Troe, J.; Ushakov, V. G.; Viggiano, A. A. *J. Phys. Chem. A* **2006**, *110*, 1491–1499.

(40) Stevens, W.; Sztáray, B.; Shuman, N.; Baer, T.; Troe, J. *J. Phys. Chem. A* **2009**, *113*, 573–582.

(41) Chesnavich, W. J.; Bass, L.; Su, T.; Bowers, M. T. *J. Chem. Phys.* **1981**, *74*, 2228–2246.

(42) Troe, J. *Z. Phys. Chem.* **2009**, *223*, 347–357.

(43) Baer, T.; Hase, W. L. *Unimolecular Reaction Dynamics: Theory and Experiments*; Oxford University Press: New York, 1996.

(44) Stevens, W. R.; Walker, S. H.; Shuman, N. S.; Baer, T. *J. Phys. Chem. A* **2010**, *114*, 804–810.

(45) Shuman, N. S.; Spencer, A. P.; Baer, T. *J. Phys. Chem. A* **2009**, *113*, 9458–9466.

(46) Ruscic, B.; Pinzon, R. E.; Morton, M. L.; Srinivasan, N. K.; Su, M.-C.; Sutherland, J. W.; Michael, J. V. *J. Phys. Chem. A* **2006**, *110*, 6592–6601.

(47) Ruscic, B.; Michael, J. V.; Redfern, P. C.; Curtiss, L. A.; Raghavachari, K. *J. Phys. Chem. A* **1998**, *102*, 10889–10899.

(48) Ruscic, B.; Litorja, M.; Asher, R. L. *J. Phys. Chem. A* **1999**, *103*, 8625–8633.

(49) Ruscic, B. Active Thermochemical Tables. In *2005 Yearbook of Science and Technology of the McGraw-Hill Encyclopedia of Science and Technology*; McGraw-Hill: New York, 2004; pp 3−7.

(50) Rossini, F. D. Assignment of Uncertainties to Thermochemical Data. In *Experimental Thermochemistry*; Rossini, F. D., Ed.; Interscience: New York, 1956.

(51) Rossini, F. D.; Deming, W. E. *J. Washington Acad. Sci.* **1939**, *29*, 416–441.

(52) Fogleman, E. A.; Koizumi, H.; Kercher, J. P.; Sztáray, B.; Baer, T. *J. Phys. Chem. A* **2004**, *108*, 5288–5294.

(53) Baer, T.; Li, Y. *Int. J. Mass Spectrom.* **2002**, *219*, 381–389.

(54) Kercher, J. P.; Stevens, W.; Gengeliczki, Z.; Baer, T. *Int. J. Mass Spectrom.* **2007**, *267*, 159–166.

(55) Bodi, A.; Johnson, M.; Gerber, T.; Gengeliczki, Z.; Sztáray, B.; Baer, T. *Rev. Sci. Instrum.* **2009**, *80*, 034101/1-034101/7.

(56) Frisch, M. J.; Trucks, G. W.; Schlegel, H. B.; Scuseria, G. E.; Robb, M. A.; Cheeseman, J. R.; Montgomery, J. A.; Vreven, T.; Kudin, K. N.; Burant, J. C.; Millam, J. M.; Iyengar, S. S.; Tomasi, J.; Barone, V.; Mennucci, B.; Cossi, M.; Scalmani, G.; Rega, N.; Petersson, G. A.; Nakatsuji, H.; Hada, M.; Ehara, M.; Toyota, K; Fukuda, R.; Hasegawa, J.; Ishida, M.; Nakajima, T.; Honda, Y.; Kitao, O.; Nakai, H.; Klene, M.; Li, X.; Knox, J. E.; Hratchian, H. P.; Cross, J. B.; Adamo, C.; Jaramillo, J.; Gomperts, R.; Stratmann, F.; Yazyev, O.; Austin, A. J.; Cammi, R.; Pomelli, C.; Ochterski, J. W.; Ayala, P. Y.; Morokuma, K.; Voth, G. A.; Salvador, P.; Dannenberg, J. J.; Zakrzewski, V. G.; Dapprich, S.; Daniels, A. D., Strain, M. C.; Farkas, Ö.; Malick, D. K.; Rabuck, A. D.; Raghavachari, K.; Foresman, J. B.; Ortiz, J. V.; Cui, Q.; Baboul, A. G.; Clifford, S.; Cioslowski, J.; Stefanov, B. B.; Liu, G.; Liashenko, A.; Piskorz, P.; Komáromi, I.; Martin, R. L.; Fox, D. J.; Keith, T.; Al-Laham, M. A.; Peng, C. Y.; Nanayakkara, A.; Challacombe, M.; Gill, P. M. W.; Johnson, B.; Chen, W.; Wong, M. W.; Gonzalez, C.; Pople, J. A. *Gaussian 03, Revision C.02*, Gaussian, Inc.: Wallingford, CT, 2004.

(57) Jacox, M. E. *J. Phys. Chem. Ref. Data* **2003**, *32*, 1–441.

(58) Friderichsen, A. V.; Radziszewski, J. G.; Nimlos, M. R.; Winter, P. R.; Dayton, D. C.; David, D. E.; Ellison, G. B. *J. Am. Chem. Soc.* **2001**, *123*, 1977–1988.

(59) Radziszewski, J. G.; Nimlos, M. R.; Winter, P. R.; Ellison, G. B. *J. Am. Chem. Soc.* **1996**, *118*, 7400–7401.

(60) Scott, A. P.; Radom, L. *J. Phys. Chem.* **1996**, *100*, 16502–16513.

(61) Meot-Ner, M.; Sieck, L. W. *J. Phys. Chem.* **1986**, *90*, 6687–6690.

(62) Meot-Ner, M.; Kafafi, S. A. *J. Am. Chem. Soc.* **1988**, *110*, 6297–6303.

(63) Gunion, R. F.; Gilles, M. K.; Polak, M. L.; Lineberger, W. C. *Int. J. Mass Spectrom. Ion. Proc.* **1992**, *117*, 601–620.

(64) Sokolov, O.; Hurley, M. D.; Wallington, T. J.; Kaiser, E. W.; Platz, J.; Nielsen, O. J.; Berho, F.; Rayez, M.-T.; Lesclaux, R. *J. Phys. Chem. A* **1998**, *102*, 10671–10681.

(65) Fielding, W.; Pritchard, H. O. *J. Phys. Chem.* **1962**, *66*, 821–823.

(66) Sergeev, Y. L.; Yu, L.; Akopyan, M. E.; Vilesov, F. I.; Kleimenov, V. I. *Opt. Spektrosk.* **1970**, *29*, 119–123.

(67) Durant, J. L.; Rider, D. M.; Anderson, S. L.; Proch, F. D.; Zare, R. N. *J. Chem. Phys.* **1984**, *80*, 1817–1825.

(68) Lifshitz, C.; Malinovich, Y. *Int. J. Mass Spectrom. Ion. Proc.* **1984**, *60*, 99–105.

(69) Stanley, R. J.; Cook, M.; Castleman, A. W. *J. Phys. Chem.* **1990**, *94*, 3668–3674.

(70) Ladacki, M.; Szwarc, M. *Proc. R. Soc. London A* **1953**, *219*, 341–352.

(71) Kwon, C. H.; Kim, H. L.; Kim, M. S. *J. Chem. Phys.* **2003**, *119*, 215–223.

(72) Chewter, L. A.; Sander, M.; Muller-Dethlefs, K.; Schlag, E. W. *J. Chem. Phys.* **1987**, *86*, 4737–4744.

(73) Muller-Dethlefs, K.; Schlag, E. W. *Annu. Rev. Phys. Chem.* **1991**, *42*, 109–136.

(74) Nemeth, G. I.; Selzle, H. L.; Schlag, E. W. *Chem. Phys. Lett.* **1993**, *215*, 151–155.

(75) Krause, H.; Neusser, H. J. *J. Chem. Phys.* **1992**, *97*, 5923–5926.

(76) Goode, J. G.; Hofstein, J. D.; Johnson, P. M. *J. Chem. Phys.* **1997**, *107*, 1703–1716.

(77) Grubb, S. G.; Whetten, R. L.; Albrecht, A. C.; Grant, E. R. *Chem. Phys. Lett.* **1984**, *108*, 420–424.

(78) Duncan, M. A.; Dietz, T. G.; Smalley, R. E. *J. Chem. Phys.* **1981**, *75*, 2118–2125.

(79) Burrill, A. B.; Chung, Y. K.; Mann, H. A.; Johnson, P. M. *J. Chem. Phys.* **2004**, *120*, 8587–8599.

(80) Johnson, P. M. *J. Chem. Phys.* **2002**, *117*, 10001–10007.

(81) Johnson, P. M. *J. Chem. Phys.* **2002**, *117*, 9991–10000.

(82) Asbrink, L.; Lindholm, E.; Edqvist, O. *Chem. Phys. Lett.* **1970**, 609–612.

(83) Peatman, W. B.; Borne, T. B.; Schlag, E. W. *Chem. Phys. Lett.* **1969**, *3*, 492–497.

(84) Brehm, B. *Z. Naturforsch. A.* **1966**, *21*, 196–209.

(85) Nicholson, A. J. C. *J. Chem. Phys.* **1965**, *43*, 1171–1177.

(86) El-Sayed, M. F. A.; Kasha, M.; Tanaka, Y. *J. Chem. Phys.* **1961**, *34*, 334–335.

(87) Wilkinson, P. G. *J. Chem. Phys.* **1956**, *24*, 917.

(88) Price, W. C.; Wood, R. W. *J. Chem. Phys.* **1935**, *3*, 439–444.

(89) Klasinc, L.; Kovac, B.; Guesten, H. *Pure Appl. Chem.* **1983**, *55*, 289–298.

(90) Turner, D. W.; Baker, C.; Baker, A. D.; Brundle, C. R. *Molecular Photoelectron Spectroscopy*; Wiley: New York, 1970.

(91) Bieri, G.; Asbrink, L. *J. Electron Spectrosc. Relat. Phenom.* **1980**, *20*, 149–167.

(92) Bieri, G.; Burger, F.; Heilbronner, E.; Maier, J. P. *Helv. Chim. Acta* **1977**, *60*, 2213–2233.

(93) Mattsson, L.; Kalsson, L.; Jadrny, R.; Siegbahn, K. *Phys. Scr.* **1977**, *16*, 221–224.

(94) Behan, J. M.; Johnstone, R. A. W.; Bentley, T. W. *Org. Mass Spectrom.* **1976**, *11*, 207–211.

(95) Dewar, M. J. S.; Worley, S. D. *J. Chem. Phys.* **1969**, *50*, 654.

(96) Baker, A. D.; May, D. P.; Turner, D. W. *J. Chem. Soc. (B)* **1968**, *1*, 22–34.

(97) Kwon, C. H.; Kim, H. L.; Kim, M. S. *J. Chem. Phys.* **2002**, *116*, 10361–10371.

(98) Lembach, G.; Brutschy, B. *J. Phys. Chem.* **1996**, *100*, 19758–19763.

(99) Gonohe, N.; Shimizu, A.; Abe, H.; Mikami, N.; Ito, M. *Chem. Phys. Lett.* **1984**, *107*, 22–26.

(100) Shinohara, H.; Sato, S.; Kimura, K. *J. Chem. Phys.* **1997**, *101*, 6736–6740.

(101) Grebner, Th. L.; Neusser, H. J. *Int. J. Mass Spectrom. Ion. Phys.* **1996**, *159*, 137–152.

(102) Smith, D. R.; Raymonda, J. W. *Chem. Phys. Lett.* **1971**, *12*, 269–276.

(103) Watanabe, K.; Nakayama, T.; Mottl, J. *J. Quant. Spectrosc. Radiat. Transfer* **1962**, *2*, 369–382.

(104) Lembach, G.; Brutschy, B. *Chem. Phys. Lett.* **1997**, *273*, 421–428.

(105) Wright, T. G.; Panov, S. I.; Miller, T. A. *J. Chem. Phys.* **1995**, *102*, 4793–4803.

(106) Ripoche, X.; Asselin, P.; Piuzzi, F.; Dimicoli, I. *Chem. Phys.* **1993**, *175*, 379–386.

(107) Potts, A. W.; Edvardsson, D.; Karlsson, L.; Holland, D. M. P.; MacDonald, M. A.; Hayes, M. A.; Maripuu, R.; Siegbahn, K.; von Niessen, W. *Chem. Phys.* **2000**, *254*, 385–405.

(108) Potts, A. W.; Lyus, M. L.; Lee, E. P. F.; Fattahallah, G. H. *J. Chem. Soc. Faraday Trans. 2* **1980**, *76*, 556–570.

(109) von Niessen, W.; Asbrink, L.; Bieri, G. *J. Electron Spectrosc. Relat. Phenom.* **1982**, *26*, 173–201.

(110) Ruscic, B.; Klasinc, L.; Wolf, A.; Knop, J. V. *J. Phys. Chem.* **1981**, *85*, 1486–1489.

(111) Baer, T.; Tsai, B. P.; Smith, D.; Murray, P. T. *J. Chem. Phys.* **1976**, *64*, 2460–2465.

(112) Holland, D. M. P.; Edvardsson, D.; Karlsson, L.; Maripuu, R.; Siegbahn, K.; Potts, A. W.; von Niessen, W. *Chem. Phys.* **2000**, *252*, 257–278.

(113) Walter, K.; Scherm, K.; Boesl, U. *J. Phys. Chem.* **1991**, *95*, 1188–1194.

(114) Bralsford, R.; Harris, P. V.; Price, W. C. *Proc. R. Soc. London A* **1960**, *258*, 459–469.

(115) Watanabe, K. *J. Chem. Phys.* **1957**, *26*, 542–547.

(116) Momigny, J.; Goffart, C.; D'or, L. *Int. J. Mass Spectrom. Ion. Phys.* **1968**, *1*, 53–68.

(117) Streets, D. G.; Ceasar, G. P. *Mol. Phys.* **1973**, 1037.

(118) Fujisawa, S.; Ohno, K.; Masuda, S.; Harada, Y. *J. Am. Chem. Soc.* **1986**, *108*, 6505–6511.

(119) Mohraz, M.; Maier, J. P.; Heilbronner, E.; Bieri, G.; Shiley, R. H. *J. Electron Spectrosc. Relat. Phenom.* **1980**, *19*, 429–446.

(120) Curtiss, L. A.; Raghavachari, K.; Redfern, P. C.; Rassolov, V.; Pople, J. A. *J. Chem. Phys.* **1998**, *109*, 7764–7776.

(121) Baboul, A. G.; Curtiss, L. A.; Redfern, P. C.; Raghavachari, K. *J. Chem. Phys.* **1999**, *110*, 7650–7657.

(122) Curtiss, L. A.; Redfern, P. C.; Raghavachari, K.; Pople, J. A. *J. Chem. Phys.* **2001**, *114*, 108–117.

(123) Ochterski, J. W.; Petersson, G. A.; Montgomery, J. A. *J. Chem. Phys.* **1996**, *104*, 2598–2619.

(124) Montgomery, J. A., Jr.; Frisch, M. J.; Ochterski, J. W.; Petersson, G. A. *J. Chem. Phys.* **1999**, *110*, 2822–2827.

(125) Montgomery, J. A.; Ochterski, J. W.; Petersson, G. A. *J. Chem. Phys.* **1994**, *101*, 5900–5909.

(126) Martin, J. M. L.; de Oliveira, G. *J. Chem. Phys.* **1999**, *111*, 1843–1856.

(127) W1U is the W1 method of Martin and Oliveria[126] as implemented in the Gaussian suite of programs, modifed to use UCCSD instead of ROCCSD for open shell systems.

(128) Karton, A.; Kaminker, I.; Martin, J. M. L. *J. Phys. Chem. A* **2009**, *113*, 7610–7620.

(129) Wood, G. P. F.; Radom, L.; Petersson, G. A.; Barnes, E. C.; Frisch, M. J.; Montgomery, J. A., Jr. *J. Chem. Phys.* **2006**, *125*, 094106/1-16.

(130) Chase, M. W. *NIST−JANAF Thermochemical Tables*; 4th ed.; American Institute of Physics: New York, 1998.

(131) Gurvich, L. V.; Veyts, I. V.; Alcock, C. B. *Thermodynamic Properties of Individual Substances*, 4th ed.; Hemisphere Publishing Co.: Bristol, PA, 1991.

(132) The partition function for nitrosobenzene is based on B3LYP/6-31G(2df,p)-optimized geometry. Except for the torsional mode, computed vibrational frequencies were scaled by 0.9661 and their contributions to the partition function were obtained by assuming the RRHO model. The contribution of the torsional mode was obtained by direct state count. The torsional potential was computed at the same level by relaxed scanning of the torsional dihedral angle, fitted to a cosine expansion [$V(\varphi) = a_1 \cos 2\varphi + a_2 \cos 4\varphi$; $a_1 = 1741.8$ cm^{-1}, $a_2 = 135.5$ cm^{-1}; $\alpha = 1.893$ cm^{-1}], scaled to match the G3X torsional barrier (2352.7 cm^{-1}, inclusive of ZPE effects of all other vibrational modes), and then numerically solved.

(133) Afeefy, H. Y.; Liebman, J. F.; Stein, S. E. *Neutral Thermochemical Data in NIST Chemistry WebBook*; NIST Standard Reference Database Number 69, retrieved from http://webbook.nist.gov/, 2008.

(134) Lias, S. G.; Bartmess, J. E.; Liebman, J. F.; Holmes, J. L.; Levin, R. D.; Mallard, W. G. *J. Phys. Chem. Ref. Data* **1988**, *17*, suppl. 1.

(135) The value of 8.32 ± 0.04 eV of Butcher et al. and the current ATcT value of 8.272 ± 0.010 eV clearly agree within their mutual uncertainties. A more detailed look at the spectrum (which is a remarkable average of 2500 scans) shows that Butcher et al. selected as the adiabatic ionization energy a value that is midway between the apparent apex of the unresolved rotational envelope (~ 8.29 eV) and the next small undulation in the spectrum (~ 8.34 eV). The overall uncertainty given by Butcher et al. is ostensibly a combination of the calibration uncertainty (apparently not larger than ± 0.02 eV) and the estimated uncertainty in selecting the location of the Q_{00} transition within the unresolved rotational envelope. While the small undulations may or may not reflect some real substructure in the rotational envelope (they curiously seem to almost repeat in the 1 ← 0 envelope), taking the apparent apex (~ 8.29 eV) as a reasonable representation of the location of the Q_{00} transition would make it coincide remarkably well with the current ATcT value.

(136) Cox, J. D.; Pilcher, G. *Thermochemistry of Organic and Organometallic Compounds*; Academic Press: London, 1970.

(137) Pedley, J. B.; Naylor, R. D.; Kirby, S. P. *Thermochemical Data of Organic Compounds*, 2nd ed.; Chapman and Hall: London, 1986.

(138) Pedley, J. B. *Thermochemical Data and Structures of Organic Compounds*; Thermodynamics Research Center: College Station, TX, 1994.

(139) Roux, M. V.; Temprado, M.; Chickos, J. S.; Nagano, Y. *J. Phys. Chem. Ref. Data* **2008**, *37*, 1855–1996.

(140) da Silva, G.; Bozzelli, J. W. *J. Phys. Chem. A* **2009**, *113*, 6979–6986.

(141) Smith, L. *Acta Chem. Scand.* **1956**, *10*, 884–886.

(142) Hartely, K.; Pritchard, H. O.; Skinner, H. A. *Trans. Faraday Soc.* **1951**, *47*, 254–263.

(143) Chernick, C. L.; Skinner, H. A.; Wadso, I. *Trans. Faraday Soc.* **1956**, *52*, 1088–1093.

(144) Kumaran, S. S.; Su, M.-C.; Michael, J. V. *Chem. Phys. Lett.* **1997**, *269*, 99–106.

(145) Lias, S. G.; Liebman, J. F.; Levin, R. D. *J. Phys. Chem. Ref. Data* **1984**, *13*, 695–808.

JP107561S